Distributed Compressive Wide-Band Spectrum Sensing

Ying Wang⋆, Ashish Pandharipande⋆, Yvan Lamelas Polo† and Geert Leus†

⋆Philips Research Europe - Eindhoven,
High Tech Campus, 5656 AE Eindhoven, The Netherlands
Email: {ying.z.wang, ashish.p}@philips.com
†Faculty of EEMCS, Delft University of Technology, The Netherlands
Email: g.j.t.leus@tudelft.nl

Abstract—We consider a compressive wide-band spectrum sensing scheme for cognitive radio networks. Each cognitive radio (CR) sensing receiver transforms the received analog signal from the licensed system in to a digital signal using an analog-to-information converter. The autocorrelation of the compressed signal is then collected from each CR at a fusion center. A compressive sampling recovery algorithm that exploits joint sparsity is then employed to reconstruct an estimate of the signal spectrum and used to make a decision on signal occupancy. We compare the performance of this distributed compressive spectrum sensing scheme with a compressive spectrum sensing scheme at a single CR and show the performance gains obtained from spatial diversity.

Index Terms—Distributed compressive sampling, Wide-band spectrum sensing, Cognitive radio, Spectrum estimation.

I. INTRODUCTION

Efficient utilization of radio spectrum has received recent attention with the explosive growth in the number of wireless applications and services and the dearth of available spectrum for licensed allocation [13]. Recent spectrum measurements have shown that large portions of licensed spectrum, notably in the VHF-UHF bands licensed to television broadcasting, are under-utilized [8], [15]. This means that at a given spatial region and time, there are frequency bands with no signal occupancy. Such empty spectrum can be available for secondary access by means of cognitive radios. Cognitive radios employ spectrum sensing to determine frequency bands that are vacant of licensed transmissions and restrict their secondary transmissions to such empty portions to meet regulatory requirements of limiting harmful interference to licensed systems.

Future cognitive radios will be capable of scanning wide bands of frequencies [1], in the order of a few GHz, and employ adaptive waveforms for transmission depending on the estimated spectrum of licensed systems. In this paper, we consider the problem of determining spectrum occupancy of licensed systems over a wide band in a cognitive radio network setting, where we have a number of CRs and a centralized fusion center that collects and processes information from individual CRs in order to make a decision on spectrum occupancy. The spectrum sensing scheme we consider is based on compressive sampling.

Compressive sampling (CS) is a method for acquisition of sparse signals at rates significantly lower than the Nyquist sampling rate; signal reconstruction is a solution to an l_1-norm optimization problem [2], [6]. In [14], [16] spectrum sensing schemes based on the principle of CS were presented for a single wide-band CR sensing receiver. In particular in [14], acquisition of the wide-band analog signal is performed using an analog-to-information converter (AIC). An AIC directly relates to the idea of sampling at the information rate of the signal. Practical approaches to the design of AICs have been considered in [10], [12]. An estimate of the original signal spectrum is then made based on CS reconstruction using a wavelet edge detector following the approach in [16]. It has however been observed that such a sensing scheme does not result in a sufficiently high detection probability at low signal-to-noise ratios (SNRs) commonly encountered in wireless channel fading conditions.

In this paper, we consider an extension of [14] applicable to a network of distributed CRs. Different CR sensing receivers acquire the same wide-band signal from the licensed system at different SNRs. The underlying signal model as such is covered by the joint sparsity model, JSM-2, considered in [7]. Signal processing at each individual CR is done as in [14] and the autocorrelation vectors of the compressed signal from the CRs are collected at the fusion center. A distributed CS algorithm based on [7] is then used to obtain an estimate of the signal spectrum.

We compare the performance of the distributed compressive spectrum sensing scheme with that of the scheme of [14] for a single CR to show the gains accrued from spatial diversity and exploiting the joint sparsity structure. We use (i) the mean squared error (MSE) between the reconstructed power spectrum density (PSD) estimate and the PSD based on Nyquist rate sampling, and (ii) the probability of detecting spectrum occupancy over the channels as performance measures.

The remainder of the paper is organized as follows. In Section II, the system model is briefly described and basic principles of CS are reviewed. We recapitulate the compressive spectrum sensing scheme of [14] in Section III that is applicable for a single CR. The distributed compressive spectrum sensing scheme is then presented in Section IV. Simulation results are shown in Section V, with conclusions drawn in Section VI.

II. PRELIMINARIES

A. System model

We consider a CR network comprising of J CRs and a centralized fusion center. We consider the frequency range of interest to be comprised of P non-overlapping contiguous channels. The bandwidth and channelization of the channels need not in general be known to the cognitive radio. Sensing is performed periodically at each CR and the results are sent to the fusion center, where a decision is made on whether or not there is a licensed signal present in each channel.

B. Compressive sampling

We shall first follow [2], [6] and [16] to review basic CS principles. Let the analog signal $x(t)$, $0 \leq t \leq T$, be represented as a finite weighted sum of basis functions (e.g., Fourier) $\psi_i(t)$ as follows

$$x(t) = \sum_{i=1}^{N} s_i \psi_i(t) \qquad (1)$$

where only a few basis coefficients s_i are much larger than zero due to the sparsity of $x(t)$. In particular, with a discrete-time CS framework, consider the acquisition of an $N \times 1$ vector $\mathbf{x} = \boldsymbol{\Psi} \mathbf{s}$, where $\boldsymbol{\Psi}$ is the $N \times N$ sparsity basis matrix and $\mathbf{s}$ an $N \times 1$ vector with $K \ll N$ non-zero (and large enough) entries s_i. It has been shown that $\mathbf{x}$ can be recovered using $M = K\mathcal{O}(\log N)$ non-adaptive linear projection measurements on to an $M \times N$ basis matrix $\boldsymbol{\Phi}$ that is incoherent with $\boldsymbol{\Psi}$ [3]. An example construction of $\boldsymbol{\Phi}$ is given by choosing elements that are drawn independently from a random distribution, e.g., Gaussian, Bernoulli. The measurement vector $\mathbf{y}$ can be written as

$$\mathbf{y} = \boldsymbol{\Phi}\mathbf{x} = \boldsymbol{\Phi}\boldsymbol{\Psi}\mathbf{s}. \qquad (2)$$

Reconstruction is achieved by solving the following l_1-norm optimization problem

$$\hat{\mathbf{s}} = \arg\min_{\mathbf{s}} \|\mathbf{s}\|_1 \quad \text{s.t.} \quad \mathbf{y} = \boldsymbol{\Phi}\boldsymbol{\Psi}\mathbf{s}. \qquad (3)$$

Linear programming techniques, e.g., basis pursuit [4], or iterative greedy algorithms [11] can be used to solve (3).

Distributed versions of CS have been considered in [5] and [7] in order to exploit the underlying correlation structures in the signal observations. The specific signal observation model of interest to us is the joint sparsity model JSM-2 [7], where the received signals have a common sparsity basis support but with different basis coefficient values. Recovery in distributed compressive sampling can be done using algorithms like simultaneous orthogonal matching pursuit (SOMP) [7].

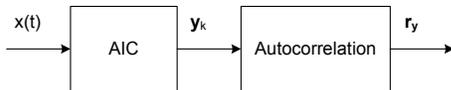## III. COMPRESSIVE SPECTRUM SENSING AT SINGLE CR

Fig. 1.   CS acquisition at individual CR sensing receiver.

We begin by describing the CS acquisition and recovery scheme for a single CR ($J = 1$) case. Figure 1 depicts the acquisition at a single CR sensing receiver. The analog baseband signal $x(t)$ is sampled using an AIC. An AIC may be conceptually viewed as an ADC operating at Nyquist rate, followed by compressive sampling. Denote the $N \times 1$ stacked vector at the input of the ADC by

$$\mathbf{x}_k = [x_{kN} \ \ x_{kN+1} \ \ \cdots \ \ x_{kN+N-1}]^T \quad k = 0, 1, 2 \ldots \quad (4)$$

and the $M \times N$ compressive sampling matrix by $\boldsymbol{\Phi}_A$. The output of the AIC denoted by the $M \times 1$ vector

$$\mathbf{y}_k = [y_{kM} \ \ y_{kM+1} \ \ \cdots \ \ y_{kM+M-1}]^T \quad k = 0, 1, 2 \ldots \quad (5)$$

is given by

$$\mathbf{y}_k = \boldsymbol{\Phi}_A \mathbf{x}_k. \qquad (6)$$

The respective $N \times N$ and $M \times M$ autocorrelation matrices of the compressed signal and the input signal vectors in (5) and (4) are related as follows

$$\mathbf{R_y} = E[\mathbf{y}_k \mathbf{y}_k^H] = \boldsymbol{\Phi}_A \mathbf{R_x} \boldsymbol{\Phi}_A^H \qquad (7)$$

where ^{H} denotes the Hermitian. The elements of the matrices in (7) are given by: $[\mathbf{R_y}]_{ij} = r_y(i-j) = r_y^*(j-i)$, $[\mathbf{R_x}]_{ij} = r_x(i-j) = r_x^*(j-i)$.

Denote the respective $2N \times 1$ and $2M \times 1$ autocorrelation vectors corresponding to (4) and (5) as follows

$$\mathbf{r_x} = [0 \ \ r_x(-N+1) \ \ \cdots \ \ r_x(0) \ \ \cdots \ \ r_x(N-1)]^T, \quad (8)$$

$$\mathbf{r_y} = [0 \ \ r_y(-M+1) \ \ \cdots \ \ r_y(0) \ \ \cdots \ \ r_y(M-1)]^T, \quad (9)$$

where the zeros are artificially inserted.

To pose the CS reconstruction in the form of (3), we need to first relate the autocorrelation vectors in (8) and (9). Note that the components of these vectors lie on the first column and row of the respective autocorrelation matrices. After some matrix algebraic operations, we obtain the following result.

$$\mathbf{r_y} = \boldsymbol{\Phi} \mathbf{r_x} \qquad (10)$$

where $\boldsymbol{\Phi}$ is given as

$$\boldsymbol{\Phi} = \begin{bmatrix} \overline{\boldsymbol{\Phi}}_A \boldsymbol{\Phi}_1 & \overline{\boldsymbol{\Phi}}_A \boldsymbol{\Phi}_2 \\ \boldsymbol{\Phi}_A \boldsymbol{\Phi}_3 & \boldsymbol{\Phi}_A \boldsymbol{\Phi}_4 \end{bmatrix}. \qquad (11)$$

Denoting the (i,j)-th element of $\boldsymbol{\Phi}_A$ by $\phi_{i,j}^*$, the $M \times N$ matrix $\overline{\boldsymbol{\Phi}}_A$ has its (i,j)-th element given by

$$[\overline{\boldsymbol{\Phi}}_A]_{i,j} = \begin{cases} 0 & i = 1, \ j = 1, \cdots, N, \\ \phi_{M+2-i,j} & i \neq 1, \ j = 1, \cdots, N, \end{cases}$$

and the $N \times N$ matrices $\boldsymbol{\Phi}_1, \boldsymbol{\Phi}_2, \boldsymbol{\Phi}_3, \boldsymbol{\Phi}_4$ are

$$\boldsymbol{\Phi}_1 = hankel([\mathbf{0}_{N\times 1}], [0 \ \ \phi_{1,1}^* \ \ \cdots \ \ \phi_{1,N-1}^*])$$

$$\boldsymbol{\Phi}_2 = hankel([\phi_{1,1}^* \ \ \cdots \ \ \phi_{1,N}^*], [\phi_{1,N}^* \ \ \mathbf{0}_{1\times(N-1)}])$$

$$\boldsymbol{\Phi}_3 = toeplitz([\mathbf{0}_{N\times 1}], [0 \ \ \phi_{1,N} \ \ \cdots \ \ \phi_{1,2}])$$

$$\boldsymbol{\Phi}_4 = toeplitz([\phi_{1,1} \ \ \cdots \ \ \phi_{1,N}], [\phi_{1,1} \ \ \mathbf{0}_{1\times(N-1)}]),$$

where $hankel(\mathbf{c}, \mathbf{r})$ is a hankel matrix (i.e., symmetric and constant across the anti-diagonals) whose first column is $\mathbf{c}$

and whose last row is $\mathbf{r}$, $toeplitz(\mathbf{c}, \mathbf{r})$ is a toeplitz matrix (i.e., symmetric and constant across the diagonals) whose first column is $\mathbf{c}$ and whose first row is $\mathbf{r}$, $\mathbf{0}_{N \times 1}$ is a column of N zeros, and $\mathbf{0}_{1 \times (N-1)}$ is a row of $N-1$ zeros.

It has been shown [16], [14] that $\mathbf{r_x}$ has a sparse representation in the edge spectrum domain. With the $2N \times 1$ discrete component vector $\mathbf{z_s}$ corresponding to the edge spectrum, we have

$$\mathbf{r_x} = \mathbf{G}\mathbf{z_s} \tag{12}$$

where $\mathbf{G} = (\boldsymbol{\Gamma}\mathcal{F}\mathcal{W})^{-1}$. The $2N \times 2N$ matrices $\mathcal{W}$ and $\mathcal{F}$ respectively denote the discrete counterparts of a wavelet-based smoothing and a Fourier transform. The $2N \times 2N$ matrix $\boldsymbol{\Gamma}$ represents a derivative operation approximated by a first-order difference and is given as

$$\boldsymbol{\Gamma} = \begin{bmatrix} 1 & 0 & \cdots & 0 \\ -1 & 1 & \cdots & 0 \\ 0 & \ddots & \ddots & \vdots \\ 0 & \cdots & -1 & 1 \end{bmatrix}.$$

Now using (12) and (10), we can formulate the CS reconstruction of the edge spectrum as an l_1-norm optimization problem

$$\hat{\mathbf{z}}_{\mathbf{s}} = \arg\min_{\mathbf{z_s}} \|\mathbf{z_s}\|_1 \quad \text{s.t.} \quad \mathbf{r_y} = (\boldsymbol{\Phi}\mathbf{G})\mathbf{z_s} \tag{13}$$

The optimization problem above is solved using the SOMP algorithm described in the following section for a single CR case. An estimate of the wide-band spectrum can now be obtained from $\hat{\mathbf{z}}_{\mathbf{s}} = [\hat{z}_{\mathbf{s}}(1)\ \hat{z}_{\mathbf{s}}(2)\ \cdots\ \hat{z}_{\mathbf{s}}(2N)]^T$ by computing a cumulative sum. The discrete components of the PSD estimate are given by

$$\hat{S}_{\mathbf{x}}(n) = \sum_{k=1}^{n} \hat{z}_{\mathbf{s}}(k). \tag{14}$$

IV. DISTRIBUTED COMPRESSIVE SPECTRUM SENSING

Let $x_j(t)$ be the wide-band analog baseband signal received at the j-th CR sensing receiver. Each CR sensing receiver processes the received signal using the acquisition scheme depicted in Figure 2(a) to obtain an autocorrelation vector of the compressed signal, as in the CS acquisition step described in Section III. For the j-th CR sensing receiver, denote the corresponding $2M \times 1$ autocorrelation vector $\mathbf{r}_{\mathbf{y},j}$; these vectors are sent to the fusion center (Actually the $M \times 1$ vector is sent since $\mathbf{r_y}$ is conjugate symmetric). The fusion center applies a SOMP algorithm to jointly reconstruct the J received PSDs $\hat{S}_{\mathbf{x},j}, j = 1, \ldots, J$ and then obtains an average PSD as shown in 2(b). The average PSD is then used to determine spectrum occupancy.

We now describe the SOMP algorithm used for reconstruction of the J PSDs. We write $\boldsymbol{\Theta} = \boldsymbol{\Phi}\mathbf{G}$ in terms of its columns

$$\boldsymbol{\Theta} = [\boldsymbol{\theta}_1\ \boldsymbol{\theta}_2\ \cdots\ \boldsymbol{\theta}_{2N}]. \tag{15}$$

Denote Ω to be the index set of all columns of the matrix $\boldsymbol{\Theta}$

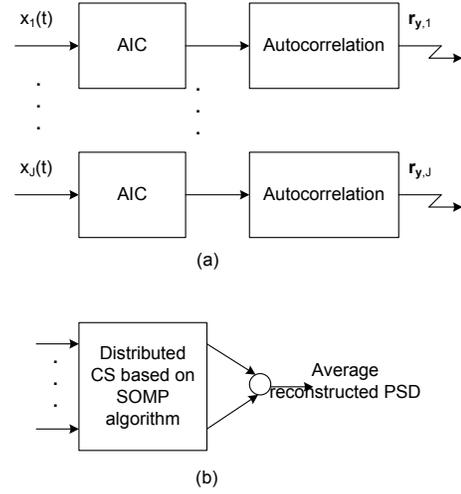$$\Omega = \{1, 2, \ldots, 2N\} \tag{16}$$

Fig. 2. (a) CS acquisition at individual CR sensing receivers, (b) Recovery at fusion center

and Ω_k to be the index set of all columns that are selected from the beginning up to step k. At the k-th iteration step, the algorithm selects a new column of the common sparse support via a two-stage selection process. In the first stage, the inner products of the current residual are examined with the remaining bases for all the signals. Based on these inner products, the search is narrowed down to a small set of potential candidates. In the second stage, the basis that provides average maximal reduction of the residual is selected. The procedure of our algorithm is described as follows:

I. Input:
  - A common dictionary $2M \times 2N$ matrix $\boldsymbol{\Theta}$.
  - A $2M \times J$ data matrix $\mathbf{R} = [\mathbf{r}_{\mathbf{y},1}\ \mathbf{r}_{\mathbf{y},2}\ \cdots\ \mathbf{r}_{\mathbf{y},J}]$ corresponding to the acquired data from the J CR sensing receivers.
  - ρ (optional) maximum number of iterations.
  - ξ (optional) threshold for convergence.

II. Output:
  - A $2N \times J$ reconstruction matrix $\mathbf{Z_s} = [\mathbf{z}_{\mathbf{s},1}\ \mathbf{z}_{\mathbf{s},2}\ \cdots\ \mathbf{z}_{\mathbf{s},J}]$ solving

$$\boldsymbol{\Theta}\mathbf{Z_s} = \mathbf{R} \tag{17}$$

  with all $\mathbf{z}_{\mathbf{s},j}$ sharing the same sparse support.

III. Procedure:
  1. Denote $\mathbf{R}^{(k)}$ as the $2M \times J$ residual matrix obtained at the k-th iteration written in terms of its columns

$$\mathbf{R}^{(k)} = [\mathbf{r}_1^{(k)}\ \mathbf{r}_2^{(k)}\ \cdots\ \mathbf{r}_J^{(k)}].$$

  Initialize the residual $\mathbf{R}^{(0)} = \mathbf{R}$, the index set $\Omega^{(0)} = \emptyset$, the selected columns $\boldsymbol{\Theta}^{(0)} = [\ ]$ (empty matrix), and the counter $k = 1$.

  2. Denote $\mathbf{c}_n^{(k)}$ as the $J \times 1$ correlation vector between the residuals and the n-th dictionary element

$$\mathbf{c}_n^{(k)} = [c_{n,1}^{(k)}\ c_{n,2}^{(k)}\ \cdots\ c_{n,J}^{(k)}]^T,$$

where

$$\mathbf{c}_n^{(k)} = |\langle (\mathbf{R}^{(k-1)})^T, \boldsymbol{\theta}_n \rangle|,$$

$n \in \Omega \backslash \Omega^{(k-1)}, \quad |\Omega \backslash \Omega^{(k-1)}| = 2N - (k-1)$.
Denote $\bar{\mathbf{c}}^{(k)}$ to be the $(2N - (k-1)) \times 1$ vector containing correlation values, $\bar{c}_n^{(k)}$, averaged over the J CRs, and given by

$$\bar{\mathbf{c}}^{(k)} = [\bar{c}_1^{(k)} \ \cdots \ \bar{c}_n^{(k)} \ \cdots \ \bar{c}_{2N-(k-1)}^{(k)}]^T,$$

where

$$\bar{c}_n^{(k)} = \frac{1}{J} \sum_{j=1}^{J} c_{n,j}^{(k)}, \quad n \in \Omega \backslash \Omega^{(k-1)}.$$

We select the columns of $\boldsymbol{\Theta}$ which have larger common inner products with the residual,

$$\bar{c}_*^{(k)} = \max\{\bar{\mathbf{c}}^{(k)}\}$$
$$\Xi^{(k)} = \{n : \bar{c}_n^{(k)} \geq \alpha \bar{c}_*^{(k)}\}$$

with α denoting the narrowing down factor taken from 0 to 1.

3. Search among the candidate set $\Xi^{(k)}$ for the item that maximizes the reduction of the average residual

$$n^{(k)} = \operatorname*{argmin}_{n \in \Xi^{(k)}} \sum_{j=1}^{J} \| \mathbf{r}_{\mathbf{y},j} - \mathbf{P}_{span\{\boldsymbol{\theta}_l \cup \boldsymbol{\theta}_n : l \in \Omega^{(k-1)}\}} \mathbf{r}_{\mathbf{y},j} \|_2, \quad (18)$$

where $\mathbf{P}_{span\{\mathbf{A}\}}$ represents the orthogonal projector onto the span of $\mathbf{A}$, which is given by

$$\mathbf{P}_{span\{\mathbf{A}\}} = \mathbf{A}\mathbf{A}^\dagger \quad (19)$$

with $\mathbf{A}^\dagger$ denoting the pseudo-inverse of matrix $\mathbf{A}$.

4. Update $\Omega^{(k)} = \Omega^{(k-1)} \cup n^{(k)}$, and $\boldsymbol{\Theta}^{(k)} = [\boldsymbol{\Theta}^{(k-1)} \ \boldsymbol{\theta}_{n^{(k)}}]$.

5. Update the residual:

$$\mathbf{R}^{(k)} = \mathbf{R} - \mathbf{P}_{span\{\boldsymbol{\theta}_l : l \in \Omega^{(k)}\}} \mathbf{R}. \quad (20)$$

6. Compare $\min \|\mathbf{r}_j^{(k)}\|_2^2, \ j = 1, 2, \ldots, J$ with a preselected limit ξ, and compare the number of selected items in $\Omega^{(k)}$ with a preselected limit ρ. If none of these limits have been reached yet then increase k by one and return to step 2.

7. Locations of nonzero coefficients of $\mathbf{Z}_s$ are listed in $\Omega^{(k)}$. The values of those coefficients are in the expansion

$$\mathbf{P}_{span\{\boldsymbol{\theta}_l : l \in \Omega^{(k)}\}} \mathbf{r}_{\mathbf{y},j} = \sum_{l \in \Omega^{(k)}} \hat{z}_{\mathbf{s},j}(l) \boldsymbol{\theta}_l \quad (21)$$

$$\tilde{\mathbf{z}}_{\mathbf{s},j} = (\boldsymbol{\Theta}^{(k)})^\dagger \mathbf{r}_{\mathbf{y},j}. \quad (22)$$

The nonzero elements of the $2N \times 1$ vector $\hat{\mathbf{z}}_{\mathbf{s},j}$ are given by those of $\tilde{\mathbf{z}}_{\mathbf{s},j}$, with the positions given by the index set $\Omega^{(k)}$, and the remaining elements are zero.

V. Performance analysis and simulation results

In this section we compare the performance of the proposed distributed spectrum sensing scheme for different numbers of CR sensing receivers. We choose $J = 1, 2$, and 5. We consider, at baseband, a wide frequency band of interest ranging from -40 to 40 MHz, containing 10 non-overlapping channels of equal bandwidth of 8 MHz. Each channel is possibly occupied by a licensed system transmission signal that uses OFDM modulation according to the DVB-T standard. Each 8 MHz OFDM symbol has 8192 frequency tones and a cyclic prefix length of 1024. The number of OFDM symbols used for spectrum sensing is 1. The over-sampling factor is 16, i.e. the sampling rate is 16×8 MHz. The occupancy ratio of the total 80 MHz band is 50%, i.e., 5 out of 10 channels are occupied by licensed transmission signals and the remaining 5 channels are unoccupied. The received signal is corrupted by additive white Gaussian noise (AWGN) with a variance of $\sigma_n^2 = 1$. The received SNRs on the 5 active channels are randomly varying from -10dB to -8dB. A Gaussian wavelet function is used for smoothing. For compressive sampling, $2N$ is 512 and the compression rate M/N is set to vary from 1% to 40%. The entries of the compressive sampling matrix $\boldsymbol{\Phi}_A$ are Gaussian distributed with zero mean and variance $1/M$. The parameters used in the joint reconstruction algorithm are $\alpha = 0.99$, $\rho = M$, and $\xi = 10^{-4}$.

MSE performance: We compute the normalized MSE of the estimated PSD, which is defined as

$$\text{MSE}^{(J)} = E\{\frac{\|\hat{\mathbf{S}}_{\mathbf{x}}^{(J)} - \mathbf{S}_{\mathbf{x}}^{(J)}\|_2^2}{\|\mathbf{S}_{\mathbf{x}}^{(J)}\|_2^2}\} \quad (23)$$

where $\mathbf{S}_{\mathbf{x}}^{(J)}$ denotes the average of the J PSD estimate vectors based on the periodogram using the signals sampled at Nyquist rate, and

$$\hat{\mathbf{S}}_{\mathbf{x}}^{(J)} = \frac{1}{J} \sum_{j=1}^{J} \hat{\mathbf{S}}_{\mathbf{x},j} \quad (24)$$

is the average of the J PSD estimate vectors based on our joint CS reconstruction scheme. We can see from Figure 3 that the signal recovery quality improves as the compression rate M/N increases and also as the number of CR nodes J increases.

Probability of Detection Performance: We evaluate the probability of detection P_d based on the averaged PSD estimate $\hat{\mathbf{S}}_{\mathbf{x}}^{(J)}$. The detection analysis to follow, strictly speaking, holds only for samples collected at Nyquist rate. We however use this as a simple way to analyze detection performance in the compressive sampling case as well. The decision of the presence of a licensed transmission signal in a certain channel is made by an energy detector using the estimated frequency response over that channel, i.e., the test statistic is

$$T_p^{(J)} = \sum_{k=(p-1)K+1}^{pK} \hat{S}_{\mathbf{x}}^{(J)}(k), \quad p = 1, 2, \ldots, 10 \quad (25)$$

where p is the channel index, k is the frequency subcarrier index, and $K = 25$ is the number of PSD samples of each
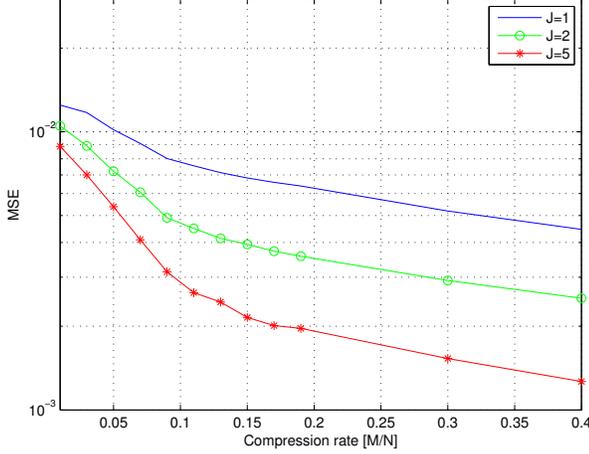
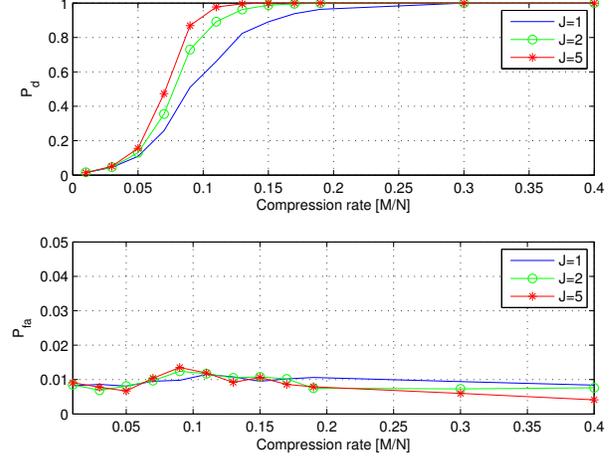Fig. 3. MSE performance versus compression rate. (SNRs of active PUs randomly varying from -10dB to -8dB.)

Fig. 4. Detection performance versus compression rate. (SNRs of active PUs randomly varying from -10dB to -8dB.)

channel. The PSD estimate at the j-th CR node can be written as

$$\hat{S}_{\mathbf{x},j}(k) = \frac{1}{Q} \sum_{q=1}^{Q} |X_{q,j}(k)|^2, \qquad (26)$$

where $X_{q,j}(k)$ is the Fourier transform of the q-th block of the received time-domain signal $x_{q,j}(n)$, j denoting the CR node index, n denoting the time sample index, each block containing $2N = 512$ time samples, and $Q = 288$ is the number of blocks. Substituting (24) and (26) into (25) we get

$$T_p^{(J)} = \frac{1}{JQ} \sum_{k=(p-1)K+1}^{pK} \sum_{j=1}^{J} \sum_{q=1}^{Q} |X_{q,j}(k)|^2 \qquad (27)$$

The decision rule is given by

$$T_p^{(J)} \underset{\mathcal{H}_0}{\overset{\mathcal{H}_1}{\gtrless}} \gamma, \quad p = 1, 2, \ldots, 10 \qquad (28)$$

where $\mathcal{H}_1$ and $\mathcal{H}_0$ denote the hypotheses of primary signal being present and absent, respectively, and γ is the decision threshold. Note that under $\mathcal{H}_0$, $T_p^{(J)}/(\sigma_n^2/(JQ))$ is centralized Chi-square distributed with $2JKQ$ degrees of freedom [9]. The false alarm probability $P_{fa}^{(J)}$ can be expressed as

$$P_{fa}^{(J)} = F_r\left(\frac{\gamma}{\sigma_n^2/(JQ)}\right) \qquad (29)$$

where F_r is the right-tail integral of the χ_{2JKQ}^2 distribution. The threshold γ is found by fixing $P_{fa}^{(J)}$ to 0.01, i.e., $\gamma = F_r^{-1}(0.01)\sigma_n^2/(JQ)$. The probability of detection $P_d^{(J)}$ is calculated as

$$P_d^{(J)} = \frac{1}{5} \sum_{p=p_1}^{p_5} Pr\{T_p^{(J)} > \gamma\} \qquad (30)$$

where $p_i, i = 1, \ldots, 5$ denote the indices of five active channels. Figure 4 shows $P_d^{(J)}$, $J = 1, 2, 5$, versus different values of compression rate M/N under a fixed $P_{fa}^{(J)}$ of 0.01.

VI. Conclusions

We presented a distributed compressive spectrum sensing scheme for cognitive radio networks. The performance of this scheme was compared with the compressive spectrum sensing scheme of [14] for a single CR, and the performance gains arising from the use of spatial diversity and joint sparsity were shown.

References

[1] D. Cabric, I. D. O'Donnell, M. S.-W. Chen and R. W. Brodersen, "Spectrum sharing radios," *IEEE Circuits and Systems Magazine*, pp. 30-45, 2006.

[2] E. Candes, J. Romberg and T. Tao, "Robust uncertainty principles: Exact signal reconstruction from highly incomplete frequency information," *IEEE Trans. on Information Theory*, vol. 52, pp. 489-509, Feb 2006.

[3] E. Candes and J. Romberg, "Sparsity and Incoherence in Compressive Sampling," *Inverse Problems*, 23(3), pp. 969-985, June 2007.

[4] S. S. Chen, D. L. Donoho, and M. A. Saunders, "Atomic decomposition by basis pursuit," *SIAM Journal on Scientific Computing*,vol. 43, No. 1, pp. 129159, 2001.

[5] S. F. Cotter, B. D. Rao, K. Engan, and K. K-Delgado, "Sparse Solutions to Linear Inverse Problems with Multiple Measurement Vectors," *IEEE Trans. on Signal Processing*, vol. 53, pp. 2477-2488, July 2005.

[6] D. L. Donoho, "Compressed Sensing," *IEEE Trans. on Information Theory*, vol. 52, pp. 1289-1306, Apr 2006.

[7] M. F. Duarte, S. Sarvotham, D. Baron, M. B. Wakin and R. G. Baraniuk, "Distributed Compressed Sensing of Jointly Sparse Signals," *Asilomar Conference on Signals, Systems and Computers*, pp. 1537-1541, 2005.

[8] Federal Communications Commission - First Report, and Order and Further Notice of Proposed Rulemaking, "Unlicensed operation in the TV broadcast bands," *FCC 06-156*, Oct. 2006.

[9] S. M. Kay, *Fundamentals of Statistical Signal Processing, Volume 2: Detection Theory*, Prentice Hall, 1998.

[10] S. Kirolos, T. Ragheb, J. Laska, M. F. Duarte, Y. Masssoud, and R. G. Baraniuk, "Practical issues in implementing analog-to-information converters," *IEEE International Workshop on System on Chip for Real Time Applications*, pp. 141-146, Dec 2006.

[11] C. La and M. Do, "Signal reconstruction using sparse tree representations," *SPIE Wavelets XI*, vol. 5914, pp. 59140W.1-59140W.11, Sept 2005.

[12] J. Laska, S. Kirolos, Y. Massoud, R. Baraniuk, A. Gilbert, M. Iwen, and M. Strauss, "Random sampling for analog-to-information conversion of wideband signals," *IEEE Dallas Circuits and Systems Workshop*, pp. 119-122, Oct 2006.

[13] National Telecommunications and Information Administration (NTIA), "FCC Frequency Allocation Chart", 2003. Available at: http://www.ntia.doc.gov/osmhome/allochrt.pdf.

[14] Y. L. Polo, Y. Wang, A. Pandharipande and G. Leus, "Compressive Wide-Band Spectrum Sensing," *International Conference on Acoustics, Speech, and Signal Processing*, To appear, 2009.

[15] D. A. Roberson, C. S. Hood, J. L. LoCicero, and J. T. MacDonald, "Spectral occupancy and interference studies in support of cognitive radio technology deployment," *IEEE Workshop on Networking Technologies for Software Defined Radio Networks*, pp. 26-35, Sept. 2006.

[16] Z. Tian and G. B. Giannakis, "Compressed sensing for wideband cognitive radios," *Proc. of the International Conference on Acoustics, Speech, and Signal Processing*, pp. IV/1357-IV/1360, Apr 2007.

[17] Q. Zhao and B. M. Sadler, "A survey of dynamic spectrum access," *IEEE Signal Processing Magazine*, pp. 79-89, May 2007.